ADVANCES IN GEODESY AND GEOINFORMATION
(formerly GEODESY AND CARTOGRAPHY)
Vol. 73, no. 2, article no. e53, 2024

https://doi.org/10.24425/agg.2023.146165

Original paper

Determining the performance of HR-GNSS and RTS geodetic techniques for Structural Health Monitoring

Guldane Oku Topal*, Burak Akpınar

Yildiz Technical Universty, Istanbul, Turkey
e-mail: guldaneoku@gmail.com; ORCID: http://orcid.org/0000-0001-7548-2276
e-mail: htata@futa.edu.ng; ORCID: http://orcid.org/0000-0002-3076-1578

*Corresponding author: Guldane Oku Topal, e-mail: guldaneoku@gmail.com

Received: 2024-01-11 / Accepted: 2024-06-11

Abstract: This study investigates the effectiveness of geodetic methods in Structural Health Monitoring (SHM), focusing on the utilization of the High-Rate Global Navigation Satellite System (HR-GNSS) and Robotic Total Station (RTS) for monitoring structural movements. Experiments were conducted on a horizontal single-axis shake table to simulate various frequencies and amplitudes. Data were analyzed using time series and Fast Fourier Transform (FFT) techniques to evaluate the performance of geodetic measurement methods in SHM studies Two applications were conducted using a single-axis shake table. In the first, the table oscillated at 0.25 Hz frequency and 20 mm amplitude, while data from a GNSS receiver on the upper table underwent processing with the TRACK module of GAMIT/GLOBK software using the kinematic post-process (KPP) GNSS technique. In the second, the reflector on the shake table moved through eight oscillations at various amplitudes and frequencies, monitored automatically with a LEICA TPS1200 RTS. Time series and FFT analyses were performed on all application data to determine oscillation frequencies and amplitudes. Method accuracy was assessed by comparing these values with data from the shake table's high-precision position sensor (Linear Variable Differential Transformer-LVDT). Results showed good agreement between HR-GNSS measurements and LVDT data, with a -1.6mm amplitude difference for KPP GNSS. Additionally, RTS measurements accurately determined frequency values, with amplitude differences ranging from 0.2 mm to 6.5 mm. Root Mean Square Error (RMSE) values for eight RTS tests, covering frequencies between 0.25-0.50 Hz and amplitudes between 4.5-73.4 mm, varied from 2.1mm to 6.3mm, reflecting performance variability across different conditions.

Keywords: Structural Health Monitoring, shake table, KPP-GNSS, Robotic Total Station

1. Introduction

Measuring the movement and shape changes in engineering structures using suitable equipment is vital. Determining deformations based on measured values and promptly taking necessary precautions to prevent potential accidents are essential aspects of engineering measurements (Im et al., 2013). Geodetic monitoring methods and deformation analysis techniques are generally used to analyze the changes in engineering structures based on periodic or continuous measurements within the scope of determined standards.

Various instruments and procedures are utilized in applications for structural health monitoring (SHM). Geodetic measurement methods have become increasingly prevalent for detecting dynamic deformations and determining the structural motion of structures such as towers, tall buildings, and long bridges (Wells, 1987). In addition to using various geodetic measurement equipment in structural observation studies, SHM applications have gained a new perspective with the developing Global Navigation Satellite Systems (GNSS) technology. Static, kinematic, real-time kinematic (RTK), and precise point positioning (PPP) GNSS can be used to accurately identify the displacements in the structures (Rizos and Han, 2003). SHM research employs a diverse range of sensors and technology. However, theodolites and high-rate global navigation satellite systems (HR-GNSS) technology are already routinely employed to identify dynamic deformations (Meng et al., 2007; Psimoulis and Stiros, 2008; Picozzi et al., 2010; Stiros and Psimoulis, 2010; Xu et al. 2017).

Numerous studies have been undertaken since the early 1980s to enhance geodetic deformation analysis and its application in civil engineering and geotechnical fields, particularly in structural observations (Im et al., 2013). In Erkaya (1987), object points were established on critical parts of the Bosphorus Bridge (towers, bridge piers, and deck), and the bridge was monitored using theodolite observations. As a result of the research and examinations, it was reported that there was no deformation in the tower and bridge piers. Another study in which the movements of the Bosphorus Bridge were monitored using geodetic equipment and theodolites is the study of Erdoğan (2006). In this study, the Bosphorus Bridge, a dynamic system, is defined by non-parametric methods in the frequency and time domain depending on the effect-response variables in the case of continuous monitoring with geodetic measurements. In studies by Kovačič and Motoh (2019), the dynamic responses of the structure were determined using RTS for the Zglavje viaduct located on the A1 highway in Slovenia. Their results showed that geodetic non-contact methods are highly effective in determining structural dynamics, thanks to technological advances in speed and continuous data capturing. There are several other studies in which deflections and oscillation frequencies of engineering structures were measured using Robotic Theodolites (Lekidis et al., 2005; Psimoulis and Stiros, 2007; Stiros and Psimoulis, 2012; Moschas and Stiros, 2014; Yu et al., 2017).

As HR-GNSS technology has advanced, real-time or post-processed relative GNSS positioning approaches have been utilized since the early 1990s. These approaches require at least two GNSS receivers to monitor the dynamic displacement of towering structures and long or short-span bridges. In their study, Lovse et al. (1995) utilized a 15-minute dataset gathered at a sampling rate of 10 Hz, employing two GNSS antennas positioned atop a tower and a GNSS receiver stationed at a reference point. This investigation aimed

to analyze the structural vibrations of the 160-meter Calgary Tower in Alberta, Canada, particularly under wind-induced loading. Their findings revealed that the tower exhibited oscillations with an amplitude of around 5 mm in the east-west axis and approximately 15 mm in the north-south axis, oscillating at a frequency of 0.3 Hz. Thus, they showed that the GNSS measurement method can determine the natural frequencies of tall structures such as the Calgary Tower. According to Çelebi and Şanlı's (2002) research of a 34-story building in San Francisco using GNSS and accelerometer, high-rise structural vibrations can be measured using a 10 Hz GNSS receiver. They emphasized that the results of the test measurements showed that GNSS is a more advantageous technology than the accelerometer for determining displacements. Moschas and Stiros (2011, 2015) conducted vibration experiments on two pedestrian bridges, utilizing GNSS and accelerometers to quantify vertical displacements. They recorded the responses created by artificially synchronized jumps with an accelerometer and GNSS and compared the amplitude and frequency results. As a result, their studies reported that only a few mm standard deviations and 3-dimensional natural frequencies up to 6-7 Hz could be determined by GNSS methods. There are more studies on the use of HR-GNSS in the observation of dams, bridges, and tall structures (Hartinger and Brunner, 1998; Erdoğan, 2006; Li et al., 2006; Meng et al., 2007; Picozzi et al., 2010; Ferreira and Branco, 2015; Gorski, 2017; Konakoglu, 2021).

Additionally, some research has been carried out to predict engineering structures' inherent frequencies and motions, simulate the high oscillations expected during probable disasters, and capture these displacements utilizing GNSS technology. Wang et al. (2012)'s study includes the experiments they carried out using a three-axis shake table and the 1 Hz interval GNSS results of the Chile earthquake in 2010. Their research compared results from accelerometers installed on a 3-axis shake table and GNSS receivers for various harmonic table motions. Their findings suggest that the accuracy of high-rate kinematic GNSS depends on antenna movement rather than the receiver sampling rate. They observed that errors in GNSS measurements were significantly larger during periods of intense shaking, coinciding with the significant accelerations and shaking experienced by GNSS receivers and antennas. In the study of Akpınar et al. (2017), in which they compared the Network RTK methods using a single-axis shake table, a series of applications were conducted to detect structural movements. In this context, sub-cm accuracies were obtained by comparing the displacements obtained due to the tests they performed by connecting to the İstanbul Su ve Kanalizasyon İdaresi (İSKİ), Continuously Operating Reference Station (CORS) and Yıldız (YLDZ) networks with the position sensor of the shake table (LVDT). There are several other studies in this area (Önen et al., 2014; Nie et al., 2016; Dindar et al., 2018; Oku Topal et al., 2023).

Another application of HR-GNSS is GNSS seismology, which is progressing in parallel with structural health studies. HR-GNSS systems precisely measure ground displacements induced by seismic activities, including earthquakes, tectonic movements, and volcanic eruptions. By continuously monitoring the positions of GNSS receivers installed across seismically active regions, researchers can capture subtle changes in ground motion with unprecedented accuracy and temporal resolution. Numerous researchers have explored the potential for HR-GNSS in seismology (Ge, 1999; Bilich et al., 2008; Li et al., 2013; Liu et al., 2014).

Analyzing the time and frequency domain is essential for evaluating structural observations. With the time series analysis, the response of engineering structures depending on the acting loads is predicted and can be described with models. With time series analysis and modeling, it is possible to understand the dynamic or time-dependent nature of the observations of a single series. However, it may be insufficient to express the responses of engineering structures as a function of time only in the time domain. This inadequacy arises from the necessity to extract crucial frequency information embedded within the signals to comprehend structural responses comprehensively.

For this reason, after examining the signals in the time domain, the signals in the frequency domain must be examined to identify the motion's frequency and amplitude values. The frequency spectrum represents the signal's frequency components and is calculated in the frequency domain. The Fast Fourier Transform (FFT) is commonly used to examine frequency-domain signals (Loewke et al., 2005; Schaal and Larocca, 2009; Erdoğan and Gülal, 2013; Yiğit et al., 2020a). FFT is an efficient tool for digital signal processing tasks such as spectrum analysis, signal frequency, and amplitude determination (Yu et al., 1993).

This paper evaluates the potential of using two different geodetic measurement methods (KPP HR-GNSS and RTS) for SHM based on two different shake table tests, including a series of experiments according to amplitude and frequency characteristics. The first test examined the HR-GNSS measurement method, widely employed in structural health monitoring studies and extensively discussed in the literature in recent years. GNSS data was collected at a frequency of 1 Hz in static mode for 45 minutes. During this period, the first 30 and the last 5 minutes remained stationary, with 10 minutes of movement in between, intended for processing using the KPP method. Collecting 30 minutes of fixed data before starting kinematic measurements is to resolve the ambiguity in GNSS measurements. During this period, the GNSS receiver remains stationary, allowing for a stable reference point to be established. This static data helps correct atmospheric and other errors introduced during motion and reduces the effects of changes in receiver position during motion (Tiryakioğlu, 2012). Then, the performance of KPP GNSS methods based on the harmonic oscillation test was evaluated by comparing LVDT displacements in frequency and time domains.

The second application tested whether the RTS could determine the oscillation by moving the shake table at different frequencies and amplitudes. For this purpose, RTS measurements were carried out with eight different frequencies and amplitudes between 0.25 Hz and 0.50 Hz. Measurement data were collected with the 1 Hz sampling frequency. The data obtained with both applications were analyzed in the time and frequency domains. First, time-dependent graphs of the displacements were created and converted into a detrended series before FFT analysis. Then, the data was subjected to FFT analysis in the frequency domain, and the peak frequencies and corresponding amplitude values were determined. These values were compared with the LVDT data of the shake table, and the accuracy of the results was determined. Two geodetic measurement methods were compared, the advantages and disadvantages of the methods were determined, and their performance in structural health monitoring studies was evaluated. The novelty of this study lies in its comprehensive evaluation of how geodetic methods, such as HR-GNSS and

RTS, can be effectively employed in SHM studies. While previous literature predominantly focused on specific structural measurement techniques targeting particular amplitude and frequency values, this study stands out by conducting eight different vibration tests covering frequencies between 0.25-0.50 Hz and amplitudes between 4.5-73.4 mm that could be encountered in various structures. By testing the capabilities of GNSS and RTS in detecting structural movements across different frequency and amplitude ranges, this research expands the understanding of their potential applications in SHM. The findings underscore the versatility of geodetic measurement methods in enhancing the monitoring of dynamic behaviors in diverse structures, thereby contributing to the advancement of SHM practices.

2. Material and methods

To determine the performance of geodetic methods (KPP and RTS) in Structural Health Monitoring, some open-field experiments were carried out with the shake table. The QUANSER Shake Table II (SHII) used in this study and the Spectra Precision SP80 GNSS Receiver (technical parameters can be found at https://spectrageospatial.com/wp-content/uploads/File-1490351515.pdf) mounted on it are shown in Figure 1a. The SP80 has been preferred in our research endeavors due to its capability as a multi-GNSS receiver, capable of collecting data at dual frequencies in high frequency. The shake table used in the experiments is an earthquake simulator with a uniaxial displacement of 95 mm, used to investigate structural dynamics. The table's maximum speed is limited to 400 mm/s, and its total stroke is 190 mm. Table displacements are determined with LVDT sensors, which provide precise position feedback integrated into the hardware (Fig. 1a). LVDTs are sensors for linear position measurement, composed of a rod-like structure with primary and secondary windings around a metal core. Movement induces voltage changes between these windings based on the core's interaction with an external magnetic field. As the core moves within this field, it induces an electromotive force (EMF) between windings, allowing direct measurement of the core's position through voltage changes. LVDT sensors can measure linear position with high precision. This makes them ideal for accurately measuring the amount and speed of vibrations or movements in vibration table tests. Therefore, they are often preferred as a reference in structural monitoring studies to determine displacement movements (Amies et al., 2018; Yiğit et al., 2020(b); Bezcioglu et al., 2023). The LVDT measures the movement of the table with a precision below ±0.01 mm at 50 samples per second (50 Hz) (Bezcioglu et al., 2022). The table is moved by an electric motor with a low vibration output capability. The shake table has an upper central part powered by a strong motor that, when loaded with a mass of 7.5 kg, can produce 2.5 g of acceleration. On two metal shafts, the upper main section moves smoothly and with low path deflection thanks to linear bearings.

The measurement results reflect horizontal displacements since the table used for measurements is a horizontal single-axis shake table. Before the measurements, the shake table was oriented towards the north so that the displacements were in a single direction. Thus, the HR-GNSS results in the first application aligned with the shake table's movement axis. Since the horizontal accuracy of GNSS is known to be approximately two and a half

times higher than its vertical accuracy (Rydlund and Densmore, 2012; ICSM, 2014; Erol and Şanlı, 2023), the expected horizontal displacement accuracy in this study is also high. This is particularly important for structures such as tall buildings, where lateral forces such as wind are more significant. For structures like bridges, however, vertical displacements are known to be more influential. This aspect will be further explored in subsequent studies focusing on vertical displacement.

The Leica TPS1200 total station (technical parameters can be found at https://secure.fltgeosystems.com/uploads/tips/documents/39.pdf) utilized in the experiments features automatic target recognition (ATR) technology, which is locked onto the prism for more precise and rapid measurements (Figure 1b). ATR technology enhances accuracy by eliminating errors associated with human factors. The measurement accuracy is 3 mm + 1.5 ppm when operating in tracking mode. The Leica GPR121 professional prism has been affixed to the shake table for the RTS tests. Positioned approximately 7 meters ahead of the shake table, the RTS has continuously monitored the prism in ATR mode throughout the oscillations. This distance was chosen based on the minimum distance measurable in ATR mode with the Leica TPS1200 total station to avoid any problems when locking it to the reflector. Data was collected with RTS at a sampling rate of 1 Hz during the measurements. In the measurements, coordinate changes in a single axis were observed on the shake table by working in a local coordinate system. The horizontal displacements of the reflector during oscillation were determined using the table's midpoint as a reference point.

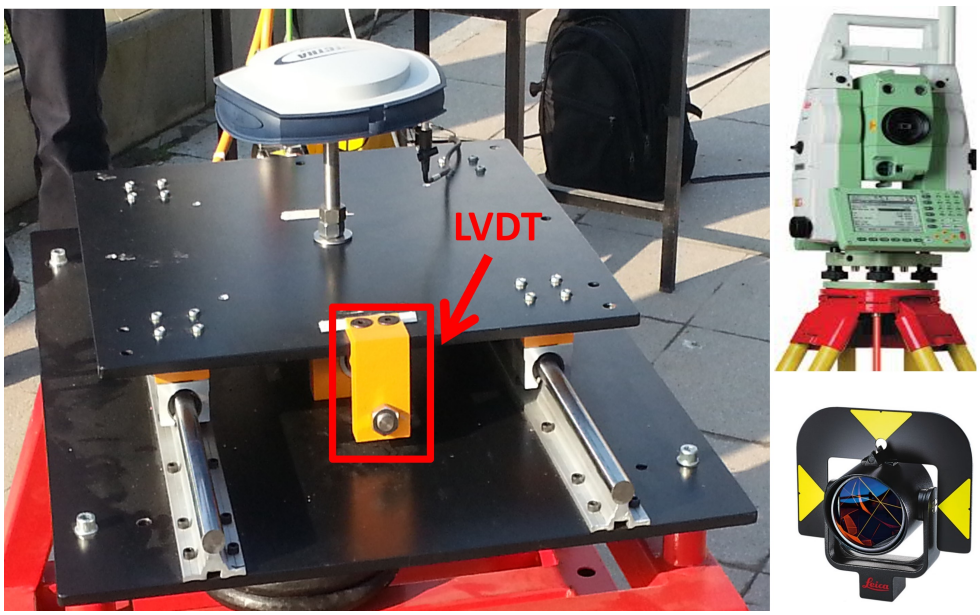

(a) (b)

Fig. 1. GNSS receiver and the shake table used in experiments (a) and the Leica TPS1200 total station and Leica GPR121 professional prism (b)

The study, conducted under open weather conditions in the garden of Yıldız Technical University Faculty of Civil Engineering, involved tests lasting approximately 2 hours. This duration included the setup phase, 45 minutes of HR-GNSS measurements, and approximately 20 minutes of RTS measurements. In KPP GNSS measurements, static data was collected for 30 minutes before starting to oscillate. Following the completion of 10-minute motion tests on the shake table, an additional 5-minute static data collection was conducted to achieve sub-centimeter accuracy in KPP measurements. GNSS data was collected using the Spectra Precision SP80 GNSS Receiver in kinematic mode and recorded at a sampling rate of 1 Hz. During the experiment, an average of 12 GPS satellites were visible, and the satellite elevation cutoff angle was set to 10°. The data acquisition interval for all methods was determined as 1 Hz. Table 1 shows the measurement period and oscillation frequencies of the GNSS and RTS tests.

Table 1. Measurement period of all events and oscillation frequencies of the shake table

Events	Observation Period of Shake Table		
GNSS (1 Hz)	Stationary	Motion Tests	Stationary
KPP	30 min	10 min (0.25 Hz)	5 min
RTS (1 Hz)	Stationary	Motion Tests	Stationary
Event 1	1 min	1 min (0.26 Hz)	–
Event 2	1 min	1 min (0.25 Hz)	–
Event 3	1 min	1 min (0.25 Hz)	–
Event 4	1 min	1 min (0.26 Hz)	–
Event 5	1 min	1 min (0.25 Hz)	–
Event 6	1 min	1 min (0.25 Hz)	–
Event 7	1 min	1 min (0.50 Hz)	–
Event 8	1 min	1 min (0.50 Hz)	1 min

2.1. Analysis in time and frequency domain

Time and frequency analyses are critical for understanding dynamic behavior and spotting potential difficulties. This process should be studied in both the time and frequency domains, and the analyses made in both domains complement each other (Erdoğan and Gülal, 2013). Time series analysis discovers structural changes over changing loads and

periods, whereas frequency analysis uncovers natural frequencies and resonance locations. For this reason, all test results on the shake table were first analyzed using time series analysis and then Fast Fourier Transform (FFT) analysis.

Time Series Analysis

Time series analysis dissects a system's time series into trends and periodic movements, aiding in defining and controlling the system. A time series collects data regularly by observing a specific outcome variable. This series emerges as successive values of a variable are recorded over time intervals (Sincich, 1996). When analyzing time series data, the initial step involves creating the series graphically in the time domain. Subsequently, the presence of a trend component within the series is assessed. A trend signifies a gradual increase or decrease in the data over successive observations, influenced by natural or human factors. A polynomial function is what is used to define a detected trend component in a series, which represents the long-term changes in the series:

$$Y\left(t_i\right)\text{Trend} = \sum_{k=1}^{m} c_k t_i^{k-1}, \tag{1}$$

where the parameters that rely on the function's degree are c_k $(k = 1, 2, \ldots, m)$. In Eq.1, $Y\left(t_i\right)Trend$ represents the trend component at a specific time point t_i while c_k denotes coefficients determining the shape and magnitude of the trend. The parameter m signifies the degree of the polynomial function, influencing the complexity of the trend model. By adjusting the coefficients c_k through regression analysis, the function captures the overall trend, aiding in the subsequent detrending process of the time series data (Erdoğan and Gülal, 2013). After the coefficients of the obtained equation are calculated by regression analysis, the detrended time series is obtained by subtracting this trend from the time series. After that, the frequency and amplitude of the series should be determined using spectral analysis. Fast Fourier Transform (FFT) converts series from the time domain to the frequency domain (Erdoğan, 2006).

Fast Fourier Transform Analysis

Spectral analysis examines the frequency domain of a time series, focusing on identifying periodic movements and relationships between observations. FFT analysis performs the time series analysis in the frequency domain. By examining the time series, the general properties of the series can be determined, but the amplitude and frequency values cannot be obtained. Therefore, the FFT transforms the time domain into the frequency domain.

The Fourier Technique's fundamental concept is the division of the signals that comprise a time series. The series should be detrended in the FFT, as in other time series. The sum of the sine and cosine functions can represent a function with period T in FFT (Sincich, 1996).

$$g(t) = a_0 + 2\sum_{k=1}^{\infty} a_k \cos\left(\frac{2\pi}{T}kt\right) + 2\sum_{k=1}^{\infty} b_k \sin\left(\frac{2\pi}{T}kt\right). \tag{2}$$

In Eq.2, the variables represent the general form of a Fourier series: $g(t)$ denotes the value of the function concerning the independent variable t, a_0 signifies the constant term

representing the mean value of the series, a_k, and b_k are the coefficients of the cosine and sine terms respectively, where k represents the number of terms in the series, and T represents the period of the series. Insignificant frequencies are removed from the function and repeated until only significant frequencies remain. Therefore, the periodic motion's peak frequency and corresponding amplitude value are determined. The study calculated all motions' amplitude and frequency values by applying FFT.

2.2. Kinematic Post-Processing (KPP)

The relative positioning (RP) technique involves determining the coordinates of points relative to a known point. The accuracy achievable through simultaneous phase or code observations on identical satellites with two receivers at different points ranges from 0.001 to 100 ppm (Kahveci and Yıldız, 2001; Eckl et al., 2001; Wang, 2015). In this method, synchronized measurements are processed together. While one receiver continuously observes at a reference station, the other makes instant or multiple epoch observations as a mobile receiver. Processing all data together allows the determination of base vectors from the reference station to new points (Kahveci and Yıldız, 2001).

For kinematic post-process (KPP) tests, 1 Hz static data was collected for 45 minutes with an HR-GNSS receiver mounted on the shake table, with the first 30 and last 5 minutes being stationary and 10 minutes in motion. Known-coordinate reference stations are essential for the KPP method, so the YLDZ continuous GNSS station installed on the Faculty of Civil Engineering roof was chosen as a reference station. The baseline length of the YLDZ reference station is approximately 40-50 meters. The Spectra Precision Ashtech Proflex 800 GNSS Receiver installed on the YLDZ pillar collects 1 Hz GNSS data, offering sub-cm accuracy (Gülal et al., 2015). The shake table oscillated at 0.25 Hz for HR-GNSS measurements and an amplitude of 20 mm. Since these initial values may vary depending on the shake table's oscillation capacity, precise results from the LVDT will be examined in the results section.

In the KPP application, the 1 Hz kinematic data on the shake table and the 1 Hz static data of the YLDZ reference station were processed with the TRACK module of the GAMIT/GLOBK software. The main reason to use Gamit Track for kinematic evaluation in this study is its well-established reputation for accuracy and reliability in kinematic processing (Yavaşoğlu et al., 2011; Tiryakioğlu, 2012; Yiğit et al., 2016). Previous studies by the authors (Oku Topal and Akpınar, 2022) and others in the field have demonstrated the effectiveness of high-rate GNSS measurements in detecting movements across various frequencies and amplitudes. For instance, Oku Topal and Akpınar (2022) achieved successful results using CSRS-PPP online software to analyze the dynamic behavior of the shake table. Similarly, Yiğit et al. (2016) compared Gamit's relative solution results with CSRS-PPP results in displacement tests conducted over varying measurement periods. They found that Gamit processing yielded approximately twice the accuracy of CSRS-PPP, which resulted in displacement differences and RMSE errors. While the PPP method is advantageous in SHM studies due to its independence from reference stations, even a slight increase in accuracy, such as a few millimeters, can be crucial in determining

structural displacements. The superiority of the KPP method over the PPP method becomes increasingly apparent as the observation period decreases. This is because the PPP method necessitates a more extended observation period to achieve coordinate accuracy and precision comparable to the relative method. Therefore, this study aimed to enhance the analysis results by leveraging the proven high location accuracy of Gamit/Track software.

GAMIT/GLOBK is a comprehensive software package developed by the Massachusetts Institute of Technology (MIT) and offers two separate academic software, GAMIT and GLOBK (King and Bock, 2003; Herring et al., 2009). GAMIT software can estimate three-dimensional coordinates, atmospheric delays, satellite orbits, and Earth rotation parameters using pseudo-range values and carrier wave phase measurements (Tiryakioğlu, 2012). It is the kinematic GNSS processing module of TRACK GAMIT software. Unlike many such programs, the system reads all data before starting the process. The distance between fixed stations and the mobile receiver must be less than 10 km to ensure precise solutions. This module employs the Melbourne-Wübbena Wide Lane observation equations to solve L1-L2 and subsequently utilizes various technical combinations to determine the L1 and L2 loops separately (Bezmenov et al., 2019; Tiryakioğlu, 2012). Station coordinates, zenith delay parameters, double-difference measurements, and satellite orbits were determined using loose prior constraints on values (Yavaşoğlu et al., 2011). The analysis utilized IGS final orbits, antenna models specified by IGS, and earth rotation parameters from IERS (International Earth Rotation and Reference Systems Service) to mitigate error sources. Table 2 outlines the processing settings of the TRACK module of the GAMIT/GLOBK utilized in this study.

Table 2. Processing strategy of the TRACK module of GAMIT/GLOBK

Processing Summary of the TRACK module of GAMIT/GLOBK	
GNSS System	GPS
Observation Processed	CodeandPhase
Elevation Cutoff	10.000 degrees
Antenna Model	SPP91564_1
Frequency	L1 and L2
Ephemerides	IGS Final
Troposphere	Saastamoinen Model
Troposphere gradients	Computed
Ionospheric effect	L1, L2 linear combination
Epoch interval	1 sec
Phase initial ambiguity	Combination of wide and narrow lane
Solid Earth Tides	Applied

3. Results and discussion

In this section, the results will be presented from different events belonging to 2 different geodetic measurement equipment (GNSS and RTS). Applying the same time series and Fourier analysis techniques to all of the data related to all events and approaches allowed us to determine the frequency and amplitude values of the movements. These studies were carried out on the LVDT data, and the results of the frequency and amplitude calculations were compared. The measurement precision of LVDT displacements was chosen as the reference value in this study since it is substantially greater than the measurement precision of all GNSS methods. According to the manufacturer's factsheet, the repeatability of LVDT measurements is stated to be below ±0.01 mm (Bezcioglu et al., 2022; Soway Tech Limited, 2024).

Additionally, Root Mean Square Errors (RMSE) of the differences in GNSS and LVDT displacements were computed to evaluate the performance of the HR-GNSS and RTS methods. Data were sampled at 50 Hz for LVDT measurements and at 1 Hz for GNSS and RTS measurements. Since LVDT results are used as a reference for frequency and amplitude values, it is crucial to include data at a higher sampling frequency in the FFT analysis. So, LVDT data were not resampled at 1 Hz to maintain accuracy in the FFT analysis. During the FFT analysis, amplitude and frequency values were calculated by specifying the sampling frequencies used for the sensors. This does not affect the results because amplitude and frequency values of the motions are utilized to compare LVDT and GNSS. On the other hand, the LVDT data have been resampled to a 1Hz sampling frequency to calculate the RMSE values of the LVDT and GNSS displacement differences.

3.1. GNSS measurements

Table 3 presents the amplitude and frequency values obtained from GNSS processing, as described in Section 2.2. Both GNSS and LVDT datasets underwent identical time series and FFT analyses to ensure comparable results. This approach aimed to ensure that any reduction in amplitude values from the analysis would equally affect both sensors. Consequently, the amplitude and frequency values of LVDT and GNSS results were computed using the exact same time series and FFT analysis procedure. Then, differences between the amplitude and frequency values derived from GNSS measurements and those from LVDT were calculated. Additionally, root mean square errors (RMSE) of the differences in GNSS and LVDT displacements were also computed to evaluate the performance of the GNSS method.

Table 3 indicates that the frequency values obtained through the GNSS approach closely align with the LVDT results, while slight discrepancies are observed in the amplitude values. Specifically, a minor difference of -1.6 mm was identified between the amplitude value derived from the KPP GNSS and that from the LVDT. In their study published in 2020a, Yiğit et al. employed HR-GNSS measurements during 12 different shake table tests. These tests covered frequencies ranging from 0.2 to 2.5 Hz and amplitudes ranging from 5 to 10 mm. By processing the GNSS data using relative

Table 3. Oscillation frequency and amplitude of GNSS processing and RMSE values of displacement differences

LVDT Results		GNSS Results		Difference		
Amplitude (mm)	Frequency (Hz)	Amplitude (mm)	Frequency (Hz)	Amplitude (mm)	Frequency (Hz)	RMSE (mm)
18.5	0.25	20.1	0.25	-1.6	0.0	3.1

processing with Leica Geo Office (LGO) software, they obtained difference values between LVDT and GNSS amplitudes in the 0.2 to 3.0 mm. In our study, the difference value of -1.6 mm obtained with an oscillation of approximately 20 mm at a frequency of 0.25 Hz is compatible with this study. Computing the mean square error values is essential to gain deeper insights and facilitate comparison with similar studies. Therefore, the disparities between displacements obtained from the KPP methods and LVDT data were computed, and subsequently, the root-mean-square error (RMSE) value of the event was calculated. The formula for RMSE is represented in Eq. 3.

$$\text{RMSE} = \sqrt{\frac{1}{n}\sum_{i=1}^{n}(y_i - \bar{y}_i)^2}. \tag{3}$$

Eq.3 calculates the square of the differences between the actual LVDT displacement and the calculated GNSS displacement values, averages these squared differences, and then computes the square root of this average. The variable n represents the number of observations, y_i represents the LVDT displacement and $\bar{y}_i$ represents the GNSS displacement. Consequently, a lower RMSE suggests that the GNSS displacement is closer to the actual values. When the RMSE values of the displacement differences are examined, it is seen that the difference between the displacements obtained from the KPP GNSS method and the LVDT displacements has a low RMSE value of 3.1 mm. In their 2020b study, Yiğit et al. utilized HR-GNSS measurements for shake table tests, encompassing frequencies ranging from 0.10 to 3 Hz and amplitudes ranging from 5 to 10 mm. Upon processing the GNSS results using kinematic PPP and PPP-AR methods, they attained maximum RMSE values of 2.9 mm when comparing the GNSS results with LVDT measurements. In their 2022 study, Oku Topal and Akpınar conducted shake table tests using HR-GNSS measurements at frequencies ranging from 0.20- 5 Hz and amplitudes ranging from 20 to 35 mm. They processed GNSS results using kinematic PPP and found maximum differences of up to 3.9 mm between GNSS results and LVDT measurements. Bezcioglu et al. (2023) performed various harmonic oscillation tests with a geodetic GNSS receiver mounted on a single-axis shake table. They compared the displacement values calculated from the GNSS with the LVDT results. They obtained a maximum of 4.4 mm RMSE for PPP processing and a maximum RMSE of 3.3 mm for relative processing. These results are also consistent with the geodetic GNSS results in our study. It can be noted that the relative improvements in the difference values are due to the high accuracy of the position provided by the Gamit software.

Results of the LVDT and KPP GNSS are shown in Figure 2 as detrended displacement time series and FFT spectra. Figure 2 shows that the KPP GNSS–derived displacements agree well with the LVDT-derived displacements. However, the KPP-GNSS displacements have some low-frequency components other than the given frequency during the show period. While the LVDT graph shows a smooth and stable displacement, the GNSS displacements fluctuate more. This discrepancy can be attributed to several factors, including environmental conditions affecting the GNSS signals, differences in sensor sensitivity between LVDT and GNSS, and the distinct measurement methods employed by each sensor. LVDT directly measures structural changes with high precision, whereas GNSS relies on satellite signals for position estimation, making it susceptible to environmental influences. A more comprehensive analysis of these differences can be conducted by examining the amplitude and frequency values derived from the FFT analysis of both LVDT and GNSS displacements. Upon examining the event's FFT spectra, it becomes apparent that the oscillation frequencies determined by LVDT and KPP-GNSS results are in perfect agreement. However, there are slight discrepancies in their respective amplitudes. The observed difference and a low-frequency component in the KPP results can be attributed to multipath effects, random noise from the carrier phase, and higher-order ionospheric errors (Shu et al., 2017).

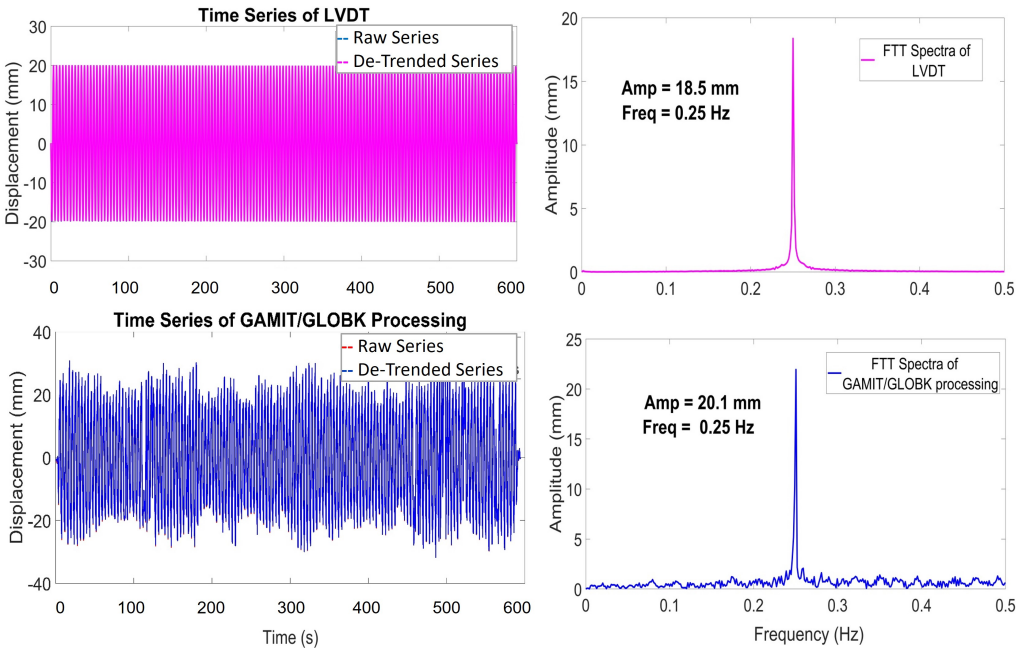

(a) (b)

Fig. 2. Time series of displacements (a) and FFT spectra for GNSS event (LVDT and TRACK module of the Gamit/Glock Processing) (b)

3.2. Robotic Total Station measurements

To determine the performance of robotic total station measurement in structural health monitoring studies, eight harmonic oscillation tests lasting 14 minutes were performed with The Leica TPS1200 RTS. The events in the selected experimental procedure were determined based on studies highlighting critical amplitude and frequencies, and also displacement values in observing engineering structures (Erdoğan, 2006; Yiğit, 2010; Panos and Stathis, 2011; Ferreira and Branco, 2015; Stiros et al., 2019). The characteristics of each oscillation experiment were predetermined, with the frequency ranging between 0.25 and 0.50 Hz (limits imposed by the specifications of the RTS used) and amplitude between 4.5 and 73 mm. Due to the Nyquist criterion, which dictates that the maximum frequency that can be determined within a 1 Hz measurement interval is 0.5 Hz, the frequencies in the experiments were capped at a maximum of 0.5 Hz. Each oscillation lasted approximately 60 seconds, corresponding to typical dynamic motions experienced by engineering structures, such as vehicles passing over a bridge or seismic events (Brownjohn, 1997; Brownjohn et al., 1997; Roberts et al., 2004). When a 60-second waiting period is included before the measurements start, it can be said that each measurement takes approximately 120 seconds.

Figure 3 shows the horizontal displacement time series derived from all events. The figure on the left shows the time series obtained from the LVDT measurements, and the right shows the time series obtained from the RTS measurements. The graph includes detrended time series graphs of both LVDT and RTS. The displacements derived from the RTS measurement appear consistent and in good agreement with those derived from the LVDT.

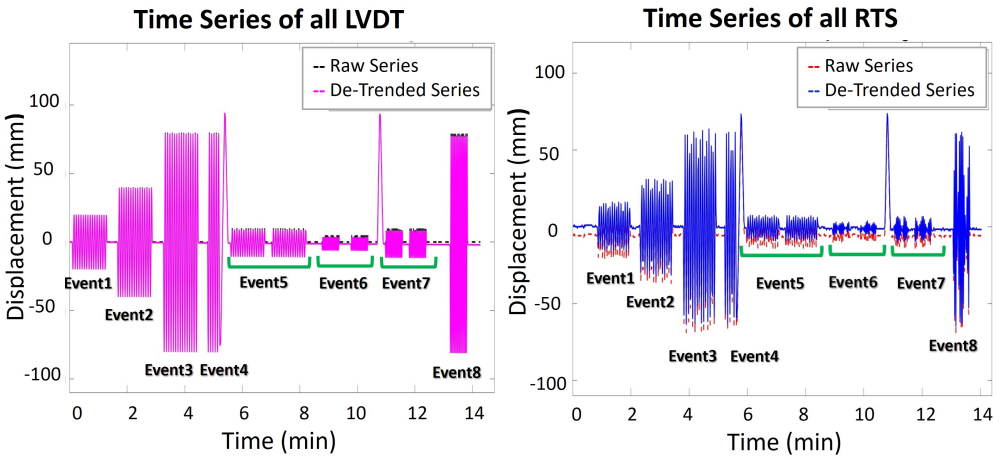

Fig. 3. Time series of displacements of LVDT and RTS for eight events

To further assess the performance of the RTS measurement, the peak frequency and amplitude values of each event were examined using the FFT technique. This analysis provided the amplitude and frequency values for eight different harmonic motions

observed by RTS. Time series and frequency analysis were also conducted on the LVDT measurement results. Table 4 presents the reference amplitude and frequency values derived from the LVDT measurements of all events. Subsequently, the amplitude and frequency values obtained from the RTS measurements were compared with the reference LVDT results, and the differences in amplitude and frequency were calculated. Additionally, the RMSE values for each event were determined by computing the mean square error between the LVDT and RTS displacements.

When Table 4 is inspected, it is seen that the frequency values of each application are obtained with high accuracy with RTS. When obtaining the amplitude values, minor deviations vary between 0.2 mm and 6.5 mm. Again, when the RMSE values are examined at the point of obtaining the displacement values with RTS, it is seen that it varies between 2.1 mm and 6.3 mm. When the table is examined, it is seen that RMSE values increase in high-frequency events with high amplitude values. Thus, increasing frequency and amplitude values have a negative impact on RTS positioning accuracy. At higher frequencies, there is an increase in measurement noise, leading to a tendency for the recorded peaks to deviate from the actual oscillation amplitude (Kijewski-Correa, 2006; Psimoulis and Stiros, 2008). Specifically, the GNSS-derived peaks tend to overestimate the amplitude of the oscillation (Fig. 2). Conversely, in the case of RTS, several cycles of oscillation are lost due to the clipping effect (Wilson, 2006; Psimoulis and Stiros, 2007; Psimoulis and Stiros, 2008; Herring et al., 2018). Consequently, only a few peaks close or bigger from the real oscillation amplitude $\pm a$ are recorded, while most recorded peaks are significantly smaller in absolute value than a (Table 4). As a result, the amplitude of recorded peaks tends to underestimate the actual amplitude of the oscillation (Panos and Stathis, 2011).

Table 4. Oscillation frequency and amplitude of each LVDT and RTS processing and RMSE values of displacement differences

	LVDT Results		RTS Results		Difference		RMSE of displacement difference (mm)
	Amplitude (mm)	Frequency (Hz)	Amplitude (mm)	Frequency (Hz)	Amplitude (mm)	Frequency (Hz)	
Event 1	15.9	0.26	17.8	0.27	-1.9	-0.01	4.1
Event 2	36.1	0.25	39.1	0.26	-3.0	-0.01	5.0
Event 3	71.6	0.25	65.1	0.26	6.5	-0.01	6.1
Event 4	73.4	0.26	67.6	0.25	5.8	0.01	6.3
Event 5	8.7	0.25	7.7	0.26	1.0	-0.01	3.5
Event 6	4.5	0.50	3.8	0.48	0.7	0.02	2.1
Event 7	6.0	0.50	5.8	0.48	0.2	0.02	2.8
Event 8	72.0	0.50	65.9	0.50	6.1	0.00	5.9

Some studies for SHM used RMSE obtained from LVDT and GNSS displacement differences to compare HR-GNSS measurement accuracy. On the other hand, in many studies, the differences in the amplitude values obtained by subjecting the LVDT and GNSS displacements to FFT analysis are used as a comparison criterion. This study

facilitated comparisons with different studies by employing two comparison criteria. Figure 4 shows the distribution of amplitude differences and RMSE values for all events. The scatterplot reveals that tests with high RMSE values also exhibit high amplitude differences. From this, it can be inferred that low RMSE in displacement values leads to consistency between the amplitude values obtained from LVDT and GNSS. When combined with the results in Table 4, it is observed that increasing amplitude and frequency values lead to higher displacement differences and, consequently, higher RMSE values determined. As a result, it can be stated that large displacements at high frequencies have a negative effect on RTS positioning accuracy.

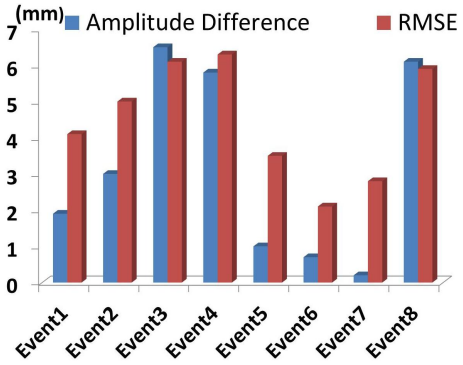

Fig. 4. RMSE and amplitude difference (between GNSS and LVDT) distribution for eight events

When the performance of RTS in detecting structural movements is studied, it is seen that frequencies up to 0.5 Hz are determined with very high accuracy. The measurements showed a maximum RMSE value of 6.3 mm, obtained in the 4th event with a maximum amplitude of 73 mm. This value falls within the Leica TPS1200 RTS's position accuracy in auto-tracking mode. Figure 5 displays all events' fast Fourier transform (FFT) spectra and the LVDT and RTS displacement time series. The determined displacements with RTS observation agree with the LVDT displacements, as shown in Figure 5.

In determining the natural frequencies of engineering structures, the sampling interval is determined according to the Nyquist criterion. According to the Nyquist criterion, sampling should be chosen as twice the maximum frequency of motion (Erdoğan, 2006). Since the robotic total station's sampling frequency is 1 Hz, it will not be possible to determine frequency values or movements greater than 0.5 Hz. The most frequently monitored structures within the scope of structural health are flexible structures where high displacements are expected, such as high-rise buildings and suspension bridges (Lovse et al., 1995; Erdoğan, 2006; Picozzi et al., 2010; Ferreira and Branco, 2015). In their study, Kwok et al. (1990) found the fundamental natural frequencies of 13 high-rise buildings in the Sydney Central Business District between 0.25 and 0.5 Hz. Çelebi (2000) monitored the dynamic behavior of a 44-store building under wind load with a GNSS receiver and determined the fundamental frequency as 0.23 Hz. The fundamental frequency of a 30-40-store high building varies between 0.25-050 Hz (Yiğit, 2016). In flexible structures such as suspension bridges, frequencies in the first mode contain about 90% of the total

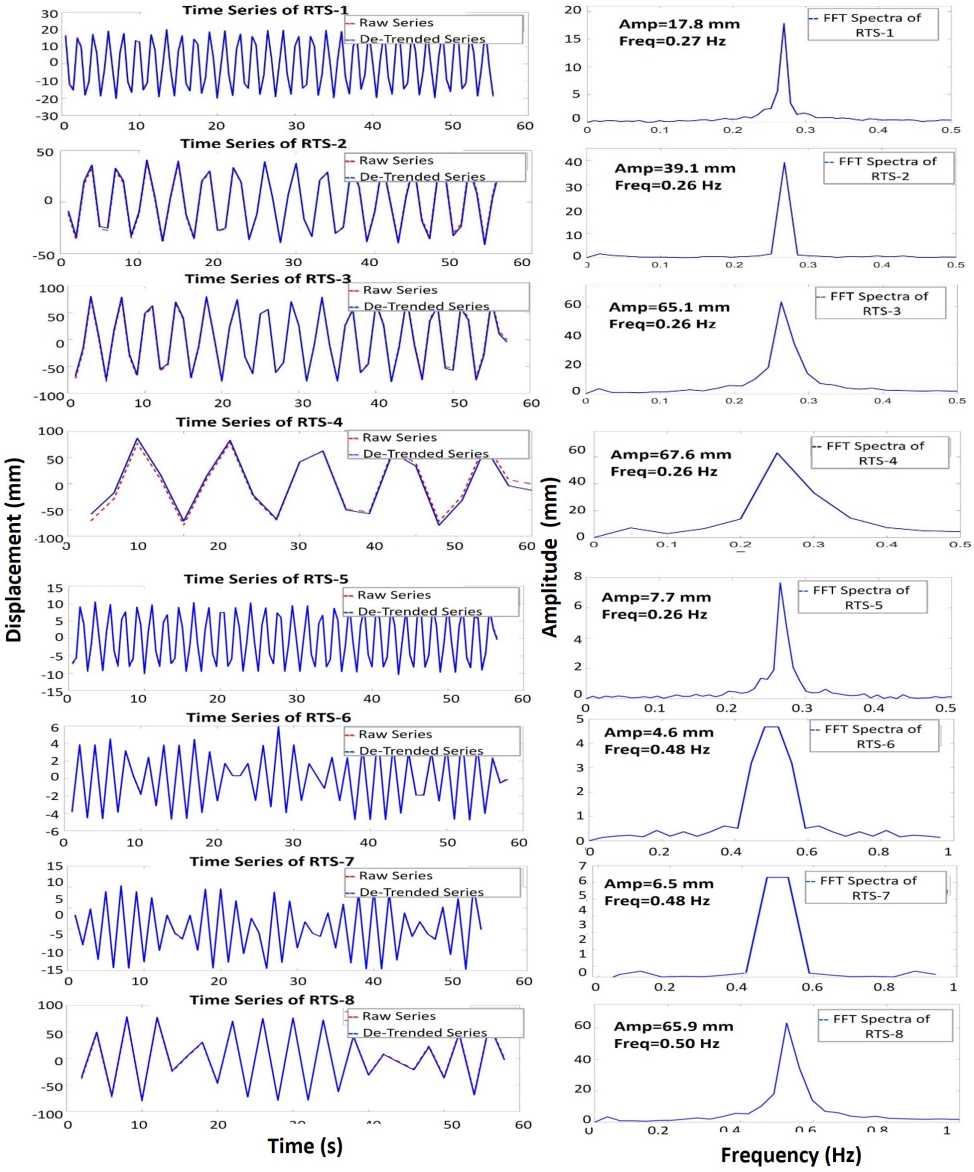

Fig. 5. Time series of displacements (left column) and FFT spectra for all events (RTS positioning) (right column)

response. The natural frequencies of wide-span suspension bridges such as the 15 March Martyrs Bridge in the first five modes vary between (0.1-0.4 Hz) (Dumanoğlu and Severn, 1985). Considering that the frequencies in the first five modes in structural observations largely reflect the structure's behavior, the RTS method may be sufficient to determine the movements of engineering structures without significant information loss.

4. Conclusion

To determine whether geodetic measurement methods can be used effectively in monitoring the behavior of engineering structures, a series of shake table tests were carried out using GNSS and RTS. With this application, an evaluation of the advantages and disadvantages, contributions, and deficiencies of geodetic measurement methods in terms of their ability to determine the dynamic parameters of the structure has been made. By applying time series analysis to all measurements, RMSE values were obtained by comparing the LVDT displacements with those obtained from the geodetic equipment. Then, the amplitude and frequency values of the movements were calculated by analyzing the series with FFT in the time domain.

The HR-GNSS measurement results show that the frequency values in the KPP method are in good agreement with the LVDT results, and the amplitude differences are -1.6 mm between KPP GNSS and LVDT results. The RMSE values have also been determined to be 3.1 mm for KPP. In addition, the oscillation frequency obtained from the FFT analysis of KPP GNSS displacements has been determined to be 100% compatible with the LVDT frequency. These results showed the usability of KPP GNSS methods in detecting natural structural behavior and monitoring the movements of structures under various factors.

When the performance of RTS measurements in monitoring structural behaviors was examined, it was determined that the frequency values were determined with high accuracy, and the amplitude differences varied between 0.2 mm and 6.5 mm. The RMSE values of eight RTS tests with frequencies between 0.25-0.50 Hz and amplitudes between 4.5-73.4 mm are examined. It could be seen that the results vary between 2.1 mm and 6.3 mm. According to the RTS results, the natural behaviors of large engineering structures can be precisely and thoroughly characterized by applying proper geodetic instrumentation. Meaningful information about the structures' natural behaviors could be determined by examining the measured observation data in the time and frequency domain. Although the ease of measurement of the GNSS method is known, using it in closed areas is impossible since it requires open-sky satellite vision. RTS observations can be an alternative for engineering structures where GNSS cannot be used in closed areas. Furthermore, the integration of both geodetic sensors allows for independent estimations and serves as a backup in case of signal outages or low-quality output, enhancing overall reliability.

In conclusion, this study contributes significantly to the field of SHM by comprehensively evaluating the effectiveness of geodetic methods, specifically GNSS and RTS. By conducting eight different vibration tests encompassing different frequencies and amplitudes, the study underscores the versatility of RTS in detecting structural movements across various types of structures. The comparison of GNSS and RTS measurements with high-precision sensors reveals their capability to capture dynamic behaviors accurately, thus highlighting their potential for widespread application in SHM practices. The findings emphasize the importance of incorporating geodetic measurement methods into SHM strategies, offering valuable insights into monitoring and assessing structural integrity. This research contributes to advancing the understanding and implementation of geodetic techniques in SHM, paving the way for future more efficient and reliable structural monitoring systems.

Author contributions

Conceptualization and methodology: G.O.T.; formal analysis and investigation: G.O.T.; writing original draft preparation: G.O.T.; writing – review and editing: G.O.T. and B.A.; supervision: B.A.

Data availability statement

The datasets used during the current study are available from the corresponding author on reasonable request.

Acknowledgements

The authors would like to thank İbrahim Tiryakioğlu and Fahri Karabulut for supporting this work.

References

Akpınar, B., Aykut, N.O., Dindar, A.A. et al. (2017). Ağ RTK GNSS Yönteminin YapıSağlığıİzleme Çalışmalarında Kullanımı, *Afyon Kocatepe University J. Sci. Eng.*, 17(2), 1030–1040.

Amies, A.C., Pretty, C.G., Rodgers, G.W. et al. (2018). Shake Table Testing of a Radar-Based Structural Health Monitoring Method. 14th IEEE/ASME International Conference on Mechatronic and Embedded Systems and Applications (MESA), Oulu, Finland, 2018, 1–6. DOI: 10.1109/MESA.2018.8449179.

Bezcioglu, M., Yigit, C.O., Mazzoni, A. et al. (2022) High-Rate (20 Hz) Single-Frequency GPS/GALILEO Variometric Approach for Real-Time Structural Health Monitoring and Rapid Risk Assessment. *Adv. Space Res.*, 70(5), 1388–1405. DOI: 10.1016/j.asr.2022.05.074.

Bezcioglu, M., Yigit, C.O., Karadeniz, B. et al. (2023). Evaluation of real-time variometric approach and real-time precise point positioning in monitoring dynamic displacement based on high-rate (20 Hz) GPS Observations. *GPS Solut.*, 27(1), 43. DOI: 10.1007/s10291-022-01381-6.

Bezmenov, I.V., Blinov, I.Y., Naumov, A.V. et al. (2019). An Algorithm for Cycle-Slip Detection in a Melbourne–Wübbena Combination Formed of Code and Carrier Phase GNSS Measurements. *Meas. Tech.*, 62, 415–421. DOI: 10.1007/s11018-019-01639-5.

Bilich, A., Cassidy, J., and Larson, K. M., (2008) GPS seismology: application to the 2002 Mw=7.9 Denali Fault Earthquake. *Bull. Seism. Soc. Am.*, 98, 593–606. DOI: 10.1785/0120070096.

Brownjohn, J.M.W. (1997). Vibration characteristics of a suspension footbridge. *J. Sound Vib.*, 202(1), 29–46. DOI: 10.1006/jsvi.1996.0789.

Brownjohn, J.M.W., Dumanoglu, A.A., Severn, R.T. et al. (1987). Ambient vibration measurements of the Humber suspension bridge and comparison with calculated characteristics. *Proc. ICE*, 2(83), 561–600. DOI: 10.1680/iicep.1987.335.

Çelebi, M. (2000). GPS in Dynamic Monitoring of Long-Period Structures. *Soil dynamic and Earthquake Engineering*, 20, 477–483.

Çelebi, M., and Sanli, A. (2002). GPS in Pioneering Dynamic Monitoring of Long-Period Structures. *Earthquake Spectra*, 18(1), 47–61. DOI: 10.1193/1.1461375.

Dindar, A.A., Akpınar, B., Gurkan, K. et al. (2018). Development Of Low-Cost Hybrid Measurement System. In 16. Europen Confrence on Earthquake Engineering, 2018, June 18–21, Greece, Thessolaniki.

Dumanoğlu, A.A. and Severn, R.T. (1985). *Asynchronous Seismic Analysis of Modern Suspension Bridges*. Part 1: Free Vibration, University of Bristol, Bristol, 1985.

Eckl, M.C., Snay, R.A., Soler, T. et al. (2001). Accuracy of GPS-derived relative positions as a function of inter-station distance and observing-session duration. *J. Geod.*, 75, 633–640. DOI: 10.1007/s001900100204.

Erdoğan, H. (2006). Mühendislik Yapılarındaki Dinamik Davranışların Jeodezik Ölçmelerle Belirlenmesi. Doctoral thesis, Yildiz Technical University,Graduate School of Science and Engineering, İstanbul, Turkey.

Erdoğan, H., and Gülal, V.E. (2013). Ambient Vibration Measurements of the Bosphorus Suspension Bridge by Total Station and GPS. *Exp. Tech.*, 37. DOI: 10.1111/j.1747-1567.2011.00723.x.

Erkaya, H. (1987). Mühendislik Yapılarındaki Deformasyonların Jeodezik Yöntemlerle Saptanmasıve Bir Model Üzerinde Uygulanması. Doctoral thesis, Yildiz Technical University,Graduate School of Science And Engineering, İstanbul, Turkey.

Erol, T., and Şanlı, D.U. (2023). Effect of Large Height Difference on Global Positioning System Solutions from a Commercially Available Software Package. *J. Surv. Eng.*, 149(1). DOI: 10.1061/(ASCE)SU.1943-5428.0000415.

Ferreira, J.G., and Branco, F. (2015). Measurement of vertical deformations in bridges using an innovative elastic cell system. *Exp. Tech.*, 39, 13–20. DOI: 10.1111/j.1747-1567.2012.00852.x.

Ge, L. (1999). *GPS seismometer and its signal extraction*. In 12th Int. Tech. Meeting, Sat. Div. of Navigation, Nashville, Tennessee, 41-51.

Gorski, P. (2017). Dynamic characteristic of tall industrial chimney estimated from GPS measurement and frequency domain decomposition. *Eng. Struct.*, 148. DOI: 10.1016/j.engstruct.2017.06.066.

Gülal, V.E., Dindar, A.A., Akpınar, B. et al. (2015). Analysis and Management of GNSS Reference Station Data. *Tech. Gazette*, 22(2), 404–414. DOI: 10.17559/TV-20140717125413.

Hartinger, H., and Brunner, F.K. (1998). Experimental detection of deformations using GPS. Proceedings of IAG Special Commission 4 Symposium Eisenstadt, 145-152.

Herring, T.A., King, R.W., and McClusky, S.C. (2009). Introduction to GAMIT/GLOBK. Release 10.35. Massachussetts Institute of Technology, Cambridge, MA, USA.

Herring, T., Gu, C., Toksöz, N., et al. (2018). GPS Measured Response of a Tall Building due to a Distant Mw 7.3 Earthquake. *Seism. Res. Lett.*, 90(1), 149–159. DOI: 10.1785/0220180147.

ICSM (Intergovernmental Committee on Surveying and Mapping) (2014). Guideline for control surveys by GNSS, Version 2.1. Canberra, Australia: ICSM.

Im, S.B., Hurlebaus, S., and Kang,Y.J. (2013). Summary Review of GPS Technology for Structural Health Monitoring. *J. Struct. Eng.*, 139, 1653-1664. DOI: 10.1061/(ASCE)ST.1943-541X.0000475.

Kahveci, M., and Yıldız, F. (2001). *Global Konum Belirleme Sistemi Teori-Uygulama*. Nobel Yayın Dağıtım: Ankara.

Kijewski-Correa, T., Kareem A, and Kochly, M. (2006). Experimental verification and fullscale deployment of Global Positioning Systems to monitor the dynamic response of tall buildings. *J. Struct. Eng.*, 132(8), 1242–1253. DOI: 10.1061/(ASCE)0733-9445(2006)132:8(1242).

King, R.W., and Bock, Y. (2003). Documentation for the GAMIT GPS Analysis Software. Release 10.1, Massachusetts Institute of Technology, Cambridge, MA, USA.

Konakoglu, B. (2021). Deformation Analysis Using Static, Kinematic and Dynamic Geodetic Deformation Models with GNSS: Deriner Dam, Artvin, Turkey. *Exp. Tech.*, 45, 645–660. DOI: 10.1007/s40799-020-00435-z.

Kovačič, B., and Motoh, T. (2019). Determination of static and dynamic response of structures with geodetic methods in loading tests. *Acta Geod. Geophys.*, 54, 243–261. DOI: 10.1007/s40328-019-00251-x.

Kwok, K.C.S., Apperley, L.W., Matesic I.J. et al. (1990). Measurement of Natural Frequency of Vibration and Damping Ratios of Tall Building and Structures. The instirution of Engineers Australia Structural Engineering Conference, Adelaide 3–5 October – Australia.

Lekidis,V., Tsakiri, M., Makra, K. et al. (2005). Evaluation of dynamic response and local soil effects of the Evripos cable-stayed bridge using multi-sensor monitoring systems. *Eng. Geo.*, 79(1–2), 43-59. DOI: 10.1016/j.enggeo.2004.10.015.

Li, X., Linlin, G., Ambikairajah, E. et al. (2006). Full-scale structural monitoring using an integrated GPS and accelerometer system. *GPS Solut.*, 10(4), 233–247. DOI: 10.1007/s10291-006-0023-y.

Li, X., Ge, M., Guo, B. et al. (2013). Temporal point positioning approach for real-time GNSS seismology using a single receiver. *Geophys. Res. Lett.*, 40, 5677–5682. DOI: 10.1002/2013GL057818.

Liu, G., Nie, Z., Fang, R. et al. (2014). Recognition of seismic phases recorded by high-rate GNSS measurements: simulation and case studies. *Chinese J. Geophys.*, 57(9), 2813–2825. DOI: 10.6038/Cjg20140908.

Loewke, K., Meyer, D., Starr, A. et al. (2005). Structural health monitoring using FFT. *Proc SPIE*, 5765, 931–935. DOI: 10.1117/12.598827.

Lovse, J.W., Teskey, W.F., Lachapelle, G. et al. (1995). Dynamic Deformation Monitoring of Tall Structure Using GPS Technology. *J. Surv. Eng.*, 121(1), 35–40. DOI: 10.1061/(ASCE)0733-9453(1995)121:1(3).

Meng, X., Dodson, A.H., and Roberts, G.W. (2007). Detecting bridge dynamics with GPS and triaxial accelerometers. *Eng. Struct.*, 29 (11), 3178–3184. DOI: 10.1016/j.engstruct.2007.03.012.

Moschas, F., and Stiros, S. (2011). Measurement of the dynamic displacements and of the modal frequencies of a short-span pedestrian bridge using GPS and an accelerometer. *Eng. Struct.*, 33(1), 10–17. DOI: 10.1016/j.engstruct.2010.09.013.

Moschas, F., and Stiros, S. (2015). Dynamic deflections of a stiff footbridge using 100-Hz GNSS and accelerometer data. *J. Surv. Eng.*, 141(4). DOI: 10.1061/(ASCE)SU.1943-5428.0000146.

Nie, Z., Zhang, R., Liu, G. et al. (2016). GNSS seismometer: Seismic phase recognition of real-time high-rate GNSS deformation waves. *J. Appl. Geophys.*, 135, 328–337. DOI: 10.1016/j.jappgeo.2016.10.026.

Oku Topal, G., and Akpınar, B. (2022). High rate GNSS kinematic PPP method performance for monitoring the engineering structures: Shake table tests under different satellite configurations. *Meas. J. Int. Meas. Conf.*, 189. DOI: 10.1016/j.measurement.2021.110451.

Oku Topal, G., Karabulut, M.F., Aykut, N.O. et al. (2023). Performance of low-cost GNSS equipment in monitoring of horizontal displacements. *Surv. Rev.,* DOI: 10.1080/00396265.2023.2179910.

Önen, Y.H., Dindar, A.A., Gülal, E. et al. (2014). Use of High-Frrequency GNSS Sebsors in Dynamıc Motions. Second European Conference on Eartquake Engineering and Seismology, 25-29 Ağustos, İstanbul.

Panos A.P., and Stathis C.S. (2011). A supervised learning computer-based algorithm to derive the amplitude of oscillations of structures using noisy GPS and Robotic Theodolites (RTS) records. *Comp. Struct.*, 92–93, 337–348. DOI: 10.1016/j.compstruc.2011.10.019.

Picozzi, M., Milkereit, C., Zulfikar, C. et al. (2010). Wireless technologies for the monitoring of strategic civil infrastructures: an ambient vibration test on the Fatih Sultan Mehmet Suspension Bridge in Istanbul, Turkey. *Bull. Earthquake Eng.*, 8, 671–691. DOI: 10.1007/s10518-009-9132-7.

Psimoulis, P., and Stiros, S. (2007). Measurement of deflections and of oscillation frequencies of engineering structures using Robotic Theodolites (RTS). *Eng. Struct*., 29(12), 3312–3324. DOI: 10.1016/j.engstruct.2007.09.006.

Psimoulis, P., and Stiros, S. (2008). Experimental Assessment of the Accuracy of GPS and RTS for the Determination of the Parameters of Oscillation of Major Structures. *Comp.-Aided Civil Infrastruct. Eng*., 23, 389–403. DOI: 10.1111/j.1467-8667.2008.00547.x.

Rizos, C., and Han, S. (2003). Reference Station Network Based RTK Systems – Concepts and Progress. *Wuhan University J. Nat. Sci.*, 8(2B), 566–574. DOI: 10.1007/BF02899820.

Roberts, G.W., Meng, X., and Dodson, A. (2004). Integrating a Global Positioning System and accelerometers to monitor deflection of bridges. *J. Surv. Eng.*, 130(2), 65–72. DOI: 10.1061/(ASCE)0733-9453(2004)130:2(65).

Rydlund, P.H., and Densmore, B.K. (2012). *Methods of practice and guidelines for using survey-grade global navigation satellite systems (GNSS) to establish vertical datum in the United States Geological Survey: U.S. Geological Survey Techniques and Methods*. In Book 11, chap. D1. Washington, DC: USGS. DOI: 10.3133/tm11D1.

Schaal, R., and Larocca, A. (2009). Measuring dynamic oscillations of a small span cable-stayed footbridge: case study using L1 GPS receivers. *J. Surv. Eng*., 135, 33–37. DOI: 10.1061/(ASCE)0733-9453(2009)135:1(33).

Shu, Y., Shi, Y., Xu, P. et al. (2017). Error analysis of high-rate GNSS precise point positioning for seismic wave measurement. *Adv. Space Res.*, 59(11), 2691–2713. DOI: 10.1016/j.asr.2017.02.006.

Sincich, T. (1996). *Business Statistics By Example.* Prentice- Hall International Editions: USA.

Soway Tech Limited (2024). LVDT Linear Position Sensors. Soway Tech Limited. Retrieved May 10, 2024, from https://www.sowaytech.com/sdp/302911/4/pd-1125040/20288307-2149358/High_precision_digital_LVDT_probe_with_0_01mm_accu.html.

Stiros, S., and Psimoulis, P. (2010). Identification of NearShore Wave Characteristics Using Robotic Total Station (RTS). *J. Surv. Eng.*, 136. DOI: 10.1061/(ASCE)SU.1943-5428.0000027.

Stiros, S., and Psimoulis, P. (2012). Response of a historical short-span railway bridge to passing trains: 3-D deflections and dominant frequencies derived from Robotic Total Station (RTS) measurements. *Eng. Struct.*, 45, 362–371. DOI: 10.1016/j.engstruct.2012.06.029.

Stiros, S., Psimoulis, P., Moschas, F. et al. (2019). Multi-sensor measurement of dynamic deflections and structural health monitoring of flexible and stiff bridges. *Bridge Struct.*, 15(1–2), 43–51. DOI: 10.3233/BRS-190152.

Tiryakioğlu, İ. (2012). GNSS Ölçüleri İle GüneybatıAnadolu'daki Blok Hareketleri Ve Gerilim Alanlarının Belirlenmesi. PhD thesis, Institute of Science,Yıldız Technical University, İstanbul, Turkey.

Wang, G., Blume, F., Meertens, C. et al. (2012). Performance of High-rate Kinematic GPS During Strong Shaking: Observations from Shake Table Tests and The 2010 Chile Earthquake. *J. Geod. Sci.*, 2(1), 15–30. DOI: 10.2478/v10156-011-0020-0.

Wang, J. (2015). Research on some research about move relative positioning techniques and method. *Atlantis Press*, 3(5), 1503–1506. DOI: 10.2991/icmmita-15.2015.277.

Wells, D.E., Beck, N., Delikaraoğlu, D. et al. (1987). *Guide To GPS Positioning*. Second Edition, Canadian GPS Associates, New Brunswick, Canada.

Wilson, J.S. (2006). Ten measurements myths. *Test Eng Manage*, 68(6), 2–3.

Xu, Y., Brownjohn, J.M.W., Hester, D. et al. (2017). Long-span bridges: Enhanced data fusion of GPS displacement and deck accelerations. *Eng. Struct.*, 147, 639–651. DOI: 10.1016/j.engstruct.2017.06.018.

Yavaşoğlu, H., Tari, E., Tüysüz, O. et al. (2011). Determining and modelling tectonic movements along the central part of the North Anatolian Fault (Turkey) using geodetic measurements. *J. Geodyn.*, 51, 339–343. DOI: 10.1016/j.jog.2010.07.003.

Yiğit, C.Ö. (2010). Yüksek Yapıların FarklıSensörler ile Tam Ölçekli İzlenmesi ve Dinamik Parametrelerin Belirlenmesi. Doctoral thesis, Selçuk University, Graduate School of Science and Engineering, Konya, Turkey.

Yiğit, C.O., Coskun, M.Z., Yavasoglu, H. et al. (2016). The potential of GPS Precise Point Positioning method for point displacement monitoring: A case study. *Meas.*, 91, 398–404. DOI: 10.1016/j.measurement.2016.05.074.

Yiğit, C.O., El-Mowafy, A., Bezcioglu, M. et al. (2020a). Investigating the effects of ultra-rapid, rapid vs. final precise orbit and clock products on high-rate GNSS-PPP for capturing dynamic displacements. *Struct. Eng. Mech.*, 73, 427–436. DOI: 10.12989/sem.2020.73.4.427.

Yiğit, C.O., El-Mowafy, A., Dindar, A.A. et al. (2020b). Investigating Performance of High-Rate GNSS-PPP and PPP-AR for Structural Health Monitoring: Dynamic Tests on Shake Table. *J. Surv. Eng.,* 147. DOI: 10.1061/(ASCE)SU.1943-5428.0000343.

Yu, Y.S. , Zou, S., and Whittemore, D. (1993). Non-parametric Trend Analysis of Water Quality Data of Rivers in Kansas. *J. Hydro.*, 150, 61–80. DOI: 10.1016/0022-1694(93)90156-4.

Yu, J., Zhu, P., Xu, B. et al. (2017). Experimental assessment of high sampling-rate robotic total station for monitoring bridge dynamic responses. *Meas.*, 104, 60–69. DOI: 10.1016/j.measurement.2017.03.014.